IEEE Access
Multidisciplinary | Rapid Review | Open Access Journal

Received April 12, 2020, accepted April 28, 2020, date of publication May 7, 2020, date of current version May 21, 2020.

Digital Object Identifier 10.1109/ACCESS.2020.2993053

Deep Learning-Based Food Quality Estimation Using Radio Frequency-Powered Sensor Mote

MINH BINH LAM[1,2], TRUNG-HAU NGUYEN[1], AND WAN-YOUNG CHUNG[1], (Senior Member, IEEE)

[1]Department of Electronic Engineering, Pukyong National University, Busan 48513, South Korea
[2]Faculty of Electrical Engineering Technology, Industrial University of Ho Chi Minh City, Ho Chi Minh City 71406, Vietnam

Corresponding author: Wan-Young Chung (wychung@pknu.ac.kr)

This work was supported by the National Research Foundation of Korea (NRF) funded by the Ministry of Science and ICT (MSIT), Korea Government under Grant 2019R1H1A2080130.

ABSTRACT In the past decades, the emerging concern about food safety has led to the increasing demand for monitoring food quality across the world. Aiming towards a novel solution for monitoring food, this study proposes a non-destructive method with self-powering capability for online food monitoring, which can be extendable to IoT applications. Furthermore, the study introduces a novel deep neural network model to predict different states of food quality based on the monitoring results. To monitor the variation in food quality, the paper proposes the detection of total volatile organic compounds (TVOCs) inside the food packages, which have been released during food deterioration. A low-power sensor mote comprised of a capacity humidity sensor and a metal-oxide (MOX) gas sensor was manufactured for this purpose. The self-powering capability of the mote is provided through an energy harvester module, which benefits from the far-field Radio Frequency Energy Harvesting (RFEH) technology. The operating frequency of the module was chosen at the 915-MHz ISM band. The analysis of the harvester performance showed that the harvester could generate 3.3-V dc with an RF input power of as low as -8 dBm, which was sufficient for the mote operation. To verify the proposed solutions, a demonstration to monitor the deterioration of packaged pork and fish was conducted in eight days under ambient and refrigerated storage conditions, using the self-developed RF-powered sensor mote. The raw variations in TVOCs were analyzed to evaluate the reliability of the proposed TVOC-based method. A one-dimensional (1-D) convolutional neural network (CNN) model was trained on the TVOCs dataset to predict different states of food quality. To investigate the applicability of the proposed 1-D CNN to multi-class determination of food quality, two other supervised machine learning algorithms using 2-D inputs, including Multilayer Perceptron (MLP), and Support Vector Machine (SVM), are studied. Their classification accuracies based on the confusion matrix are identified and compared.

INDEX TERMS Convolutional neural network (CNN), food quality prediction, radio-frequency energy harvesting, total volatile organic compounds, multilayer perceptron (MLP), support-vector machine (SVM).

I. INTRODUCTION

In recent years, food safety has become a critical issue all over the world. In 2017, WHO (World Health Organization) reported that the number of people becoming ill from food-borne diseases every year was 600 million [1]. Approximately 420,000 people were said to be killed due to consuming contaminated food in one year, also by that report. These facts present a challenge in monitoring food quality for the determination of food conditions to protect human health.

Various methods have been applied for food monitoring. Traditional and observable methods that examine the physical structure of the foods like texture [2], tenderness, flavor, juiciness, and color yield uncertain results and have a probability of contaminating the food by touching the samples. Other approaches detect microorganisms [3] and count their concentration in food samples [4], based on the concept that food products, especially those which are highly perishable such as fish and meat, are spoiled due to the growth of harmful microorganisms [5]. These methods require direct contact with the inspected sample, which may destruct the sample.

The associate editor coordinating the review of this manuscript and approving it for publication was Jie Tang.

This work is licensed under a Creative Commons Attribution 4.0 License. For more information, see https://creativecommons.org/licenses/by/4.0/

Therefore, this has driven attention towards non-invasive or non-destructive techniques for monitoring food quality. Hyperspectral imaging technologies that inspect the changes in color or texture of the sample have wider prospects with the latest advances in image processing over the past few decades [6], [7]. Other sensing-based techniques aim to measure the biochemical changes of the environment surrounding the food sample, particularly the odors released by the sample using multisensory-based devices such as electronic noses [8]. Such systems, though highly reliable, require complex configurations of associated devices and time-consuming sampling methods.

Other than these methods, this paper proposes a non-destructive and simply configured solution to monitor food quality by tracking the total volatile organic compounds (TVOCs) released from food. The difference between this solution and the existing monitoring methods is that it requires a simpler configuration, which is feasibly implemented with a battery-less system for online food monitoring. The concept behind this idea is that different volatile gases are generated as a result of a chemical or enzymatic reaction of different types of microorganisms during food deterioration [8]–[10]. In other words, this study utilizes TVOCs as an indicator of monitoring food quality.

Furthermore, this paper aims to show the feasibility of implementing the proposed method of food quality monitoring without batteries. Although many advanced battery technologies have been recently developed, they still present some limitations such as toxic chemicals from the batteries, or the requirement of periodic replacement and maintenance. Energy harvesting technologies thus become the focus of research as a battery replenishment solution [11]–[14]. A variety of sources of energy to harvest has been studied, including but not limited to solar, wind [15], mechanical vibration [16], and RF signals [17].

For the application of food monitoring, we propose using the far-field RF Energy Harvesting (RFEH) technology owing to its advantages such as fewer requirements for regular maintenance and cost-saving ability [17]. Compared to near-field RFEH, it is considered as an efficient method for remotely charging low-power sensor devices [18]. In particular, the far-field technique allows the receiver to extract the energy from the electric field of propagated radio waves at a longer distance, which can be several meters, from the power transmitter than the near-field [17], [18]. In addition, this technology usually utilizes the unlicensed ISM (Industrial – Scientific – Medical) radio bands from low frequency (LF) to super high frequency (SHF). Among these bands, ultra-high frequency (UHF) power transmission is considered as an efficient replacement for the batteries [17]. Especially, the 868-950 MHz bands are widely used not only in research [19], [20] but also in commercial products (Powercast, STMicroelectronics to name a few). This paper thus chose the 915-MHz band for the design and operation of the proposed system.

To verify the proposed methods, we developed a self-powered sensor mote to wirelessly track the changes in TVOCs. A novel energy harvester module was integrated into the mote to harvest the energy from a dedicated RF transmitter. Specifically, two orthogonal antennas, one for harvesting energy and the other for data transmission, were proposed to improve the ability of simultaneously harvesting energy and transferring data. With the proposed configuration, it is shown in the paper that the mote can harvest sufficient power to measure and transfer multi-sensing data, including temperature, relative humidity, and TVOC concentration, without the need for any external power supply. Figure 1 shows the conceptual model of the RF-powered food quality tracking system.

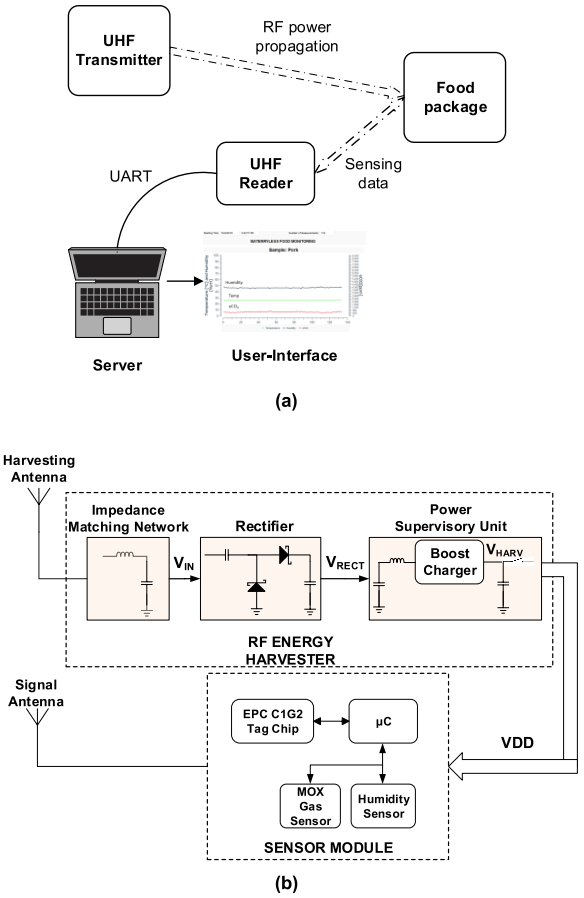

FIGURE 1. The proposed RF-powered food quality tracking system: (a) The conceptual model; (b) The block diagram of the RF-powered sensor mote.

Based on the monitored results, a classification model was developed to detect different states of food quality. In this paper, three supervised learning algorithms, including Convolutional Neural Network (CNN), Multilayer Perceptron (MLP), and Support Vector Machine (SVM), have been deployed. With the emergence of deep learning technology in recent years, CNN is the first choice to be investigated for multi-class food quality estimation in this study. One of the distinct advantages of CNN is that the convolutional layers can naturally extract inherent properties of the input data such as mean and variance, while such kinds of information

can only be provided using the feature extraction process in conventional neural networks [21]. This feature can hence simplify the pre-processing procedures of the input data. The reason behind this fact is that CNN provides an effective technique to handle any data type (i.e., one-dimensional, two-dimensional, three-dimensional data) by using kernel filters.

CNN was first known as a popular approach for image analysis, hence it usually required two- or three-dimensional input data that were the channels, the widths, and/or the heights of the images [22], [23]. Soon after, CNN has been shown to be well applied in the analysis of time- or frequency-varying signals. Particularly, a CNN model was used to classify electroencephalography (EEG) signals [24]. The inputs were the recorded EEG samples and corresponding sampling time. In [25], a CNN structure was introduced to classify five classes of steady-state visual evoked potential (SSVEP) frequencies. Again, this network required a two-dimensional map between the channels and the frequencies as its inputs.

Different than the previous works, this study aims to examine the applicability of one-dimensional (1-D) CNN to multi-class determination of food quality. To do so, the developed CNN model adopts an array of time-varying TVOC data, which is the main proposed indicator of tracking food quality, as its inputs. For assessing the performance of the proposed 1-D CNN structure, we study two other classification algorithms using two-scalar inputs, including MLP and SVM. The former was selected owing to the fact that it is the most popular conventional artificial neural network in classification problems [26], [27]. The latter was chosen owing to its good classification performance among the conventional machine learning algorithms, such as Linear Discriminant Analysis (LDA), and its wide applications [28], [29].

We summarize the contributions of this study as below:

- A food monitoring solution is proposed that is non-invasive and simply configured by tracking the TVOC concentrations released by the food;
- A battery-free sensor mote is developed that is able to be integrated with the proposed non-invasive food monitoring solution for online food quality tracking. The mote utilizes an RF energy harvester operating at the UHF band of 915 MHz. To verify its operation, the mote is examined in a demonstration of food monitoring under ambient and refrigerated storage conditions;
- Integrated with the non-invasive food monitoring solution, a new detection kernel based on 1D-CNN is proposed to compose a complete food spoilage detection model. The model classifies the freshness of food based on the measurement data of the proposed battery-less monitoring system. To investigate the applicability of 1-D CNN in the problem of multi-class categorization of food quality, we compare the classification results of the 1-D CNN with those of MLP and SVM classifiers.

The rest of the paper is organized as follows. Section II describes the design of the RF-powered sensor mote, the demonstration of the proposed RF-powered food quality tracking system under different storage conditions, and the structures of three investigated classification models. Section III discusses the demonstration results and the classification performances of these models. The comparison results of these models are shown in the same section. The last section involves our discussions and conclusions.

II. MATERIAL AND METHODS

A. THE RF-POWERED SENSOR MOTE

Figure 1 illustrates the components of the proposed RF-powered sensor mote. The power necessary for the mote operation is supplied from the RF energy harvester, while the food quality is monitored by the sensor module. The operational frequency of the mote is at the UHF band of 915 MHz.

1) THE RF ENERGY HARVESTER

In this study, the RFEH technology was used to provide the self-powering capability to the sensor mote. The concept of RFEH is that it converts the radio waves from an RF transmitter into electrical signals [17]. Therefore, an antenna is critical to induce the electric field radiated from the transmitter into an alternating current. In particular, a dipole antenna was developed in this paper owing to its omnidirectional property, which is necessary for energy harvesting [30]. To capture as much energy as possible, its return loss was targeted to be lower than -20 dB. Additionally, its input impedance was designed at 50 ohms for the ease of impedance matching. The FR4 material was chosen as the substrate of the antenna with 1.8 mm-thickness. All designs were carried out using ANSYS HFSS software (ANSYS, Inc., USA).

Figure 2 shows the prototype and the performance of the designed dipole antenna. An SMA connector was mounted onto the antenna prototype to measure its performance using a network analyzer. Parametric analyses were conducted to optimize the dimensions of the antenna to satisfy the above-mentioned goals, which were 0.8 mm wide and 138.76 mm long with the 0.8-mm gap between two arms. To compensate for the differences between designing and fabricating, a shunt inductor was integrated to achieve a practical 50-Ω input impedance. Consequently, the measured return loss agreed well with the simulated metric of the proposed antenna (Figure 2b).

Especially in this paper, a novel array of two orthogonal dipole antennas, one for energy harvesting (EH antenna) and the other for wireless communication (signal antenna), was proposed for simultaneously performing these functions. The concept of featuring two orthogonal antennas with different functions was previously introduced in [31] and [32]. Using parametric analyses, we found that orthogonally polarizing two dipole antennas at their centers enhanced the performance of the EH antenna, as shown in Figure 2c. The simulated return loss of the EH antenna, if put in the array, was found at -24.57 dB, which was improved compared to its performance if standing alone (-23.39 dB).

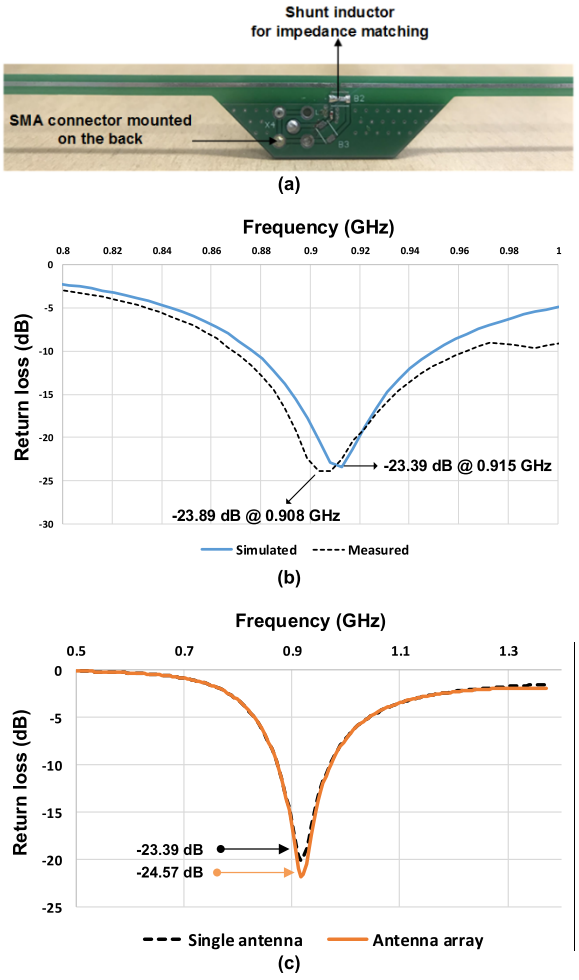

FIGURE 2. Antenna performance: (a) Antenna prototype; (b) Simulated and measured return loss of the antenna; (c) Simulated return loss of the EH antenna, if standing alone (single antenna), versus its return loss if placed in the proposed antenna array.

The next functional block of the harvester was the rectifier, which converts the ac signal into a useful dc voltage sufficient to the sensor module. There are a variety of rectification topologies studied over years in the field of RFEH, including the Greinacher and Dickson multipliers [33], [34]. The latter, however, are more appropriate in the far-field RFEH [18]. Hence, the Dickson topology was chosen for this research.

The main challenge in harvesting RF energy is the free-space path loss of the transmitter, which leads to the attenuation of the power strength. The Friis equation expresses the relationship between the transmitted (P_t) and received (P_r) power with the distance R between the power transmitter and the receiver, as follows:

$$P_r = P_t G_t G_r \left(\frac{\lambda}{4\pi R}\right)^2, \tag{1}$$

where G_r and G_t are the gains of receiving and transmitting antennas, respectively, and λ is the wavelength of the operating frequency.

The equation shows that the power strength decreases at the rate of the square of the distance. With multi-path fading, it falls off at a much faster rate, even $1/R^4$ [17]. To overcome this issue, multi-stage multipliers are widely used to generate the required dc voltage level. However, they are bulky and suffer more power loss due to the power drops on more rectifying devices, degrading their performance [17].

Therefore, this paper utilized a Dickson-style single-stage rectifier as shown in Figure 1. Schottky diodes (HSMS-285C, Avago Technologies, USA) were selected as the rectifying components owing to their low turn-on voltage (150 mV), which is the most critical metric in rectifier design [17]. The stage capacitor C_C was chosen following this constraint:

$$\frac{1}{2\pi C_C R_L} \ll f_0, \tag{2}$$

where f_0 was the operating frequency and R_L was the load resistance. With $R_L = 15$ kΩ (Section II.A.2), C_C was selected at 33 pF. In addition, a good impedance matching network between the EH antenna and the rectifier to maximize the power transferred from the antenna to the rectifier was obtained with an L-type matching network, following the method described in [19].

The last component of the harvester was the power supervisory unit. Instead of using multi-stage multiplication to generate a sufficient voltage from the low rectifying voltage, we adopted a low-power boost charger (BQ25570, Texas Instruments, USA) owing to its low quiescent current (500 nA) and low required input power (15 μW). From an input voltage as low as 330 mV, the chip can step it up to a useful voltage level from 2.2 V – 5.5 V. Moreover, the MPPT technology available in the boost charger allowed the harvester module to maximize the power extracted from the energy source [35].

To ensure smooth power delivery to the load, a storage capacitor C_{store} is essential. In this paper, a specific power management scheme was developed for power delivery to the load. The harvested power was released to the load as soon as the voltage over C_{store} reached a high threshold V_H, and was disrupted when it dropped to a low threshold V_L. A low-leakage load switch (TPS22860, Texas Instruments, USA) was used to implement the proposed scheme. The low and high thresholds were chosen to be 2.8 V and 3.3 V, respectively.

With the proposed power management scheme, the load is operational during the dropping phase of the voltage over C_{store} (V_{HARV}). Therefore, C_{store} must be large enough for at least one operational phase of the load, the sensor module in this case. In other words, the lower bound of C_{store} can be calculated based on the power consumption of the load during one phase of the load operation using (3), given by:

$$C_{store} = \frac{I_{ave} \times \Delta T}{\Delta V}, \tag{3}$$

with ΔT the duration of one operational phase of the sensor module, I_{ave} the average current consumption of the module

during ΔT, and ΔV the expected voltage drop over C_{store} during ΔT. For the worst case, $\Delta V = V_H - V_L$.

2) THE SENSOR MODULE

For a simple low-cost, and low-power hardware implementation, a single gas sensor that is able to detect a wide range of VOCs is required. The CCS811 gas sensor (ams AG, Austria) was chosen owing to its low power consumption (19 μA at sleep mode) [36]. In addition, a low-power humidity sensor (HDC1080, Texas Instruments, USA) was integrated to monitor the environment inside the food packages.

The MSP430FR5969 microcontroller (Texas Instruments, USA) was chosen for processing the sensing data and controlling the module operation owing to its ultra-low power characteristic. The module wirelessly sent the sensing data to a UHF reader (ams AG, Austria) using the SL900A tag chip (ams AG, Austria). This wireless communication complied with the EPC Radio-Frequency Identity Protocols Generation-2 [37].

The sensing data were stored at an ultra-low-power microcontroller (MSP430FR5969, Texas Instruments, USA) and sent to a UHF tag chip (SL900A, ams AG, Austria) via the Serial Peripheral Interface (SPI) for the wireless communication with a UHF reader (ams AG, Austria) afterwards. The communication was compliant with the EPC Radio-Frequency Identity Protocols Generation-2 [37].

TABLE 1. Current consumption profile of the sensor module.

Mode	Average current consumption (mA)	Duration (ms)
Active	13.1	27
Transmission	12.05	42
Sleep	0.23	220

To satisfy the shortage of power during its operation, we proposed three functional modes of the module. The active mode was the state that the module made measurements. In the transmission mode, only two components including the tag and the microcontroller functioned. Lastly, the sleep mode was programmed to remain the most vital functions of microcontroller where all other devices are inactive. Table 1 lists the current consumed by these modes and their corresponding durations, measured at 3.3-V supply power. It was found that the duration ΔT of one operational phase of the module was 289 ms, and the average current I_{ave} consumed by the module was 3.2 mA, which was equivalent to a 15-kΩ resistor.

3) ENERGY HARVESTING PERFORMANCE

To evaluate the energy harvesting capability of the mote, in addition to the antenna performance which was discussed earlier, the RF-to-DC conversion efficiency (PCE) [17] was investigated.

The efficiency is defined as the ratio of the output power P_{dc} of the rectifier to the input RF power P_{in}, given as:

$$PCE = \frac{P_{dc}}{P_{in}} \times 100\%. \quad (4)$$

To obtain this metric, at first, the harvesting antenna was connected with a spectrum analyzer (N9320A, Keysight Technologies, USA) to identify P_{in} at a specific distance d from the transmitter. Second, the harvester module was placed at the same distance d and the output voltage of the rectifier was measured by a voltmeter. The output power P_{dc} was then calculated. In this experiment, a 3-W power transmitter (Powercast, USA) was used as the power source of the module. The distance d varied from 0.1 to 4 m.

As shown in Figure 3, the simulated and measured efficiency curves of the RF energy harvester module share similar behaviors. The simulated efficiency was obtained using the ADS (Advanced Design System) software. The input RF power was measured within the range $[-8, 8]$ dBm. The largest measured rectifying voltage was 6.3 V corresponding to 8 dBm of the input RF power, resulting in the RF-to-DC efficiency of 52%. Moreover, the results showed that at $d = 4$ m ($P_{in} = -8$ dBm), the harvester generated an output voltage of 480 mV and correspondingly an output power of 15.36 μW. These levels were sufficient for the BQ25570 to start its function [35]. In other words, the proposed RF harvester module could harvest the RF energy at 4 m from the transmitter.

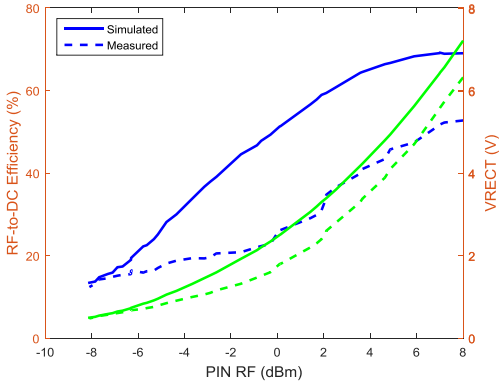

FIGURE 3. Rectifying voltage and RF-to-DC conversion efficiency of the RF energy harvester with respect to the input RF power. The green curves show the rectifying voltage, and the blue curves represent the efficiency.

4) EVALUATION OF THE RF-POWERED SENSOR MOTE OPERATION

Figure 4a shows the self-developed prototype of the sensor mote. An experiment to evaluate its operation was conducted following the paradigm in Figure 1. The distance between the transmitter and the mote was chosen at 4 meters. The storage capacitor C_{store} was the BestCap 6.8-mF super-capacitor (AVX, USA), which followed the lower bound determined by (3).

Figure 4b displays the waveform responses of the self-powered sensor mote during its operation, recorded by

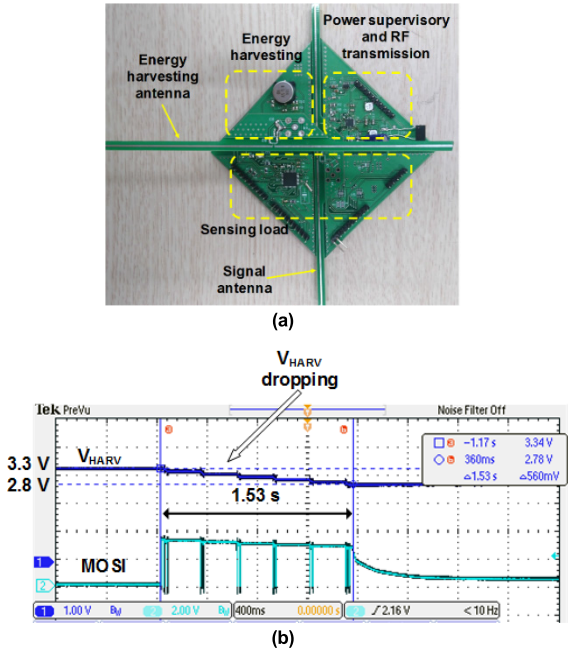

FIGURE 4. Evaluation of the proposed RF-powered sensor mote: (a) The prototype of the mote; (b) Waveform signals of the mote. The blue signal is the output voltage V_{HARV} of the harvester. The green signal represents the data signal (MOSI – master out slave in) from the microcontroller to the SL900A tag chip.

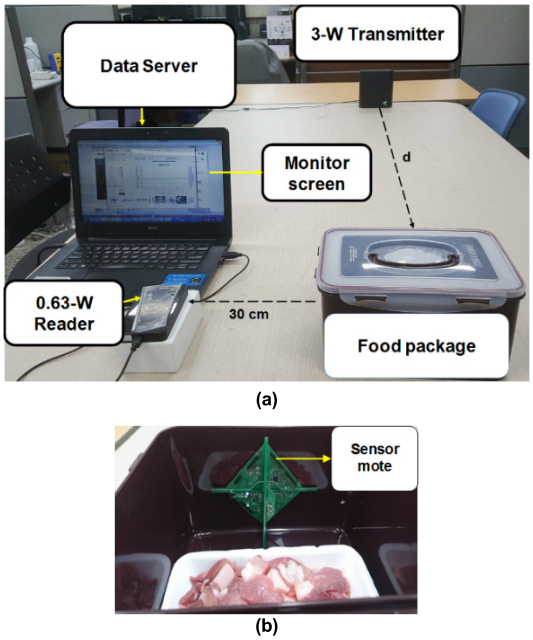

FIGURE 5. The demonstration of the RF-powered food quality tracking system: (a) System setup. The reader was from ams AG, Austria; (b) The food package integrated with the sensor mote.

an oscilloscope. As expected, after reaching 3.3 V the output voltage of the harvester dropped to 2.2 V when fed to the sensor module. During this duration, the mote measured and sent the sensing data from the microcontroller to the SL900A tag chip via the MOSI (master out slave in) wire six times as shown in Figure 4b. When $V_{HARV} = 2.8$ V, the module stopped functioning; the data signal dropped to 0 V. The results showed that the sensor mote could take measurements six times before the power was exhausted without any external power supply.

B. DEMONSTRATION OF THE RF-POWERED FOOD QUALITY TRACKING SYSTEM

To validate the feasibility of the tracking system, we conducted a demonstration of monitoring the quality of food using the proposed system. Two kinds of meat, pork (chops) and fish with 300 grams of each, were examined in 8 days under ambient and refrigerator temperatures. The developed sensor mote was placed inside the food packages to track the changes in the storage environment. The packages were sealed by silicone to ensure no gas released during the food deterioration. Figure 5 shows a practical demonstration of the pork sample under ambient storage temperature. Although the distance between the transmitter and the sensor mote could be extended up to 4 meters as discussed earlier, it was configured at 1 m at furthest for the reliable operation of the mote. The charging time of the harvester, hence, was about 4.89 minutes for one operational duration of the mote.

C. PREDICTIVE MODELS OF FOOD QUALITY ESTIMATION

In this study, deep neural networks are used for the task of multi-class food quality estimation. Although deep learning was already adopted in previous studies to analyze physical signals [24], [25], most of them required 2-D input features for the classification problem. Other than those studies, this paper investigates the performance of deep learning in food quality estimation using 1-D input. To verify the applicability of the proposed 1-D CNN model, we examine two more classification algorithms using 2-D inputs based on MLP and SVM.

1) ONE-DIMENSIONAL CNN MODEL

Figure 6 shows the proposed structure of the model. It includes three major layers: an input, N_H hidden layers, and an output. The input layer consists of two convolutional layers. As previously mentioned, the featured input was the 1-D time-varying TVOCs. In particular, n-min TVOC data (with n the data lengthd in minutes), each of which was termed an input sample, were used to be fed to the convolutional layers using five 2-point filter kernels.

Two hidden layers of 500 and 3 nodes, respectively, were fully connected to each other. It is worth noting that the second hidden layer was added for 3-D observation of the classified data. ReLu (Rectified Linear Unit) was used as the activation function of the first, while Softplus was chosen as that of the second layer. To prevent over-fitting, the dropping-out rates of the convolutional layers were configured at 10%, while that of the first hidden layer was 30%.

The output layer consisted of four nodes corresponding to four classes. The Softmax function was selected as its

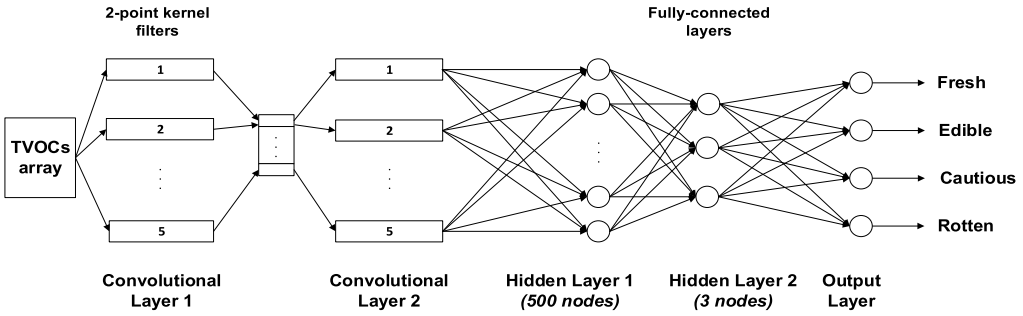

FIGURE 6. Structure of the proposed 1-D CNN model for food quality prediction.

activation function. The function takes an N-dimensional input vector of real numbers and exponentially converts it into the same dimensional vector of real numbers within the range of (0,1). The standard Softmax function $f_i(x)$ is expressed as:

$$f_i(x) = \frac{e^{x_i}}{\sum_{k=1}^{N} e^{x_k}}, \quad i = 1, \ldots, N, \tag{5}$$

The network adopted backpropagation as an optimization method to update the weights of the model. The method is aimed to find the optimized weights that best fit the model with the training dataset. For each neuron, its output y is defined as a function of the weighted sum of all its inputs x:

$$y = f\left(\sum_{j=1}^{N} w_j x_j\right), \tag{6}$$

where f is the activation function that the neuron takes, N is the number of the inputs coming to the node, and w_j is the weight on the connection from the inputs to node j.

To measure the performance of the network, cross entropy was selected as the loss function at the output of the network. In the multi-class classification problem, the overall loss of the model is the sum of the separate loss of each class label per observation, which is given as follows:

$$L = -\sum_{c=1}^{M} y_{x,c} \log\left(f_{x,c}\right), \tag{7}$$

with M the number of classes to be classified, $y_{x,c}$ the binary indicator (0 or 1) if class label c is correct for observation x, and $f_{x,c}$ the predicted probability that observation x is in class c, which is the output of the Softmax activation function. Moreover, three-fold cross-validation was implemented for statistically evaluating the performance of the model.

2) MLP MODEL

In addition to the proposed 1-D CNN, an MLP-based neural network was adopted to compare their classification results, specifically in food quality estimation. This MLP model utilized two scalars as its input, one is TVOCs and the other is the storage temperature, which had been implied as another important indicator to monitor food quality [38].

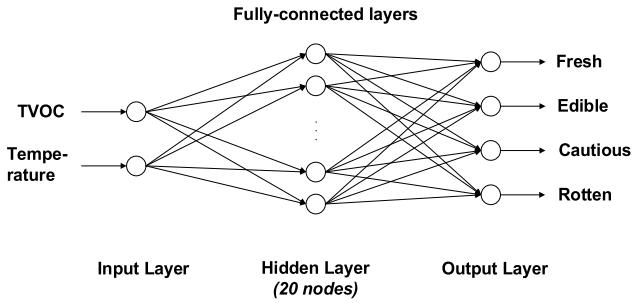

FIGURE 7. Structure of the proposed 2-D MLP model for food quality prediction.

Figure 7 shows the structure of the proposed four-class MLP model. The model comprises a single hidden layer with 20 nodes. The Softmax function was chosen as the activation function of these hidden neurons. Similar to the evaluation of the CNN model, cross-entropy loss and three-fold cross- validation were used to evaluate the classification performance of the MLP classifier.

3) SVM MODEL

Similarly, the input features of the proposed SVM classifier were the storage temperature and the TVOCs. The four-class classification problem was solved using the one-vs-one strategy with six binary SVM classifiers. In particular, the label "0" was assigned to a class, and the label "1" was assigned to another class in each classifier. Alternately, these models were trained to categorize each class. The nonlinear radial-basis kernel was adopted for this model.

4) LABELING DATA

In supervised machine learning, the input data must be labeled before being trained. This section describes how the input features of the CNN and SVM classifiers were labeled, or how the collected samples were defined, for training.

Currently, to the best of the authors' knowledge, there has been no global standard for food quality because different food types suffer from different spoilage rates at different storage conditions. Therefore, we considered the recommendation of the U.S. Food and Drug Administration (FDA) for refrigerator and freezer storage of food products [39].

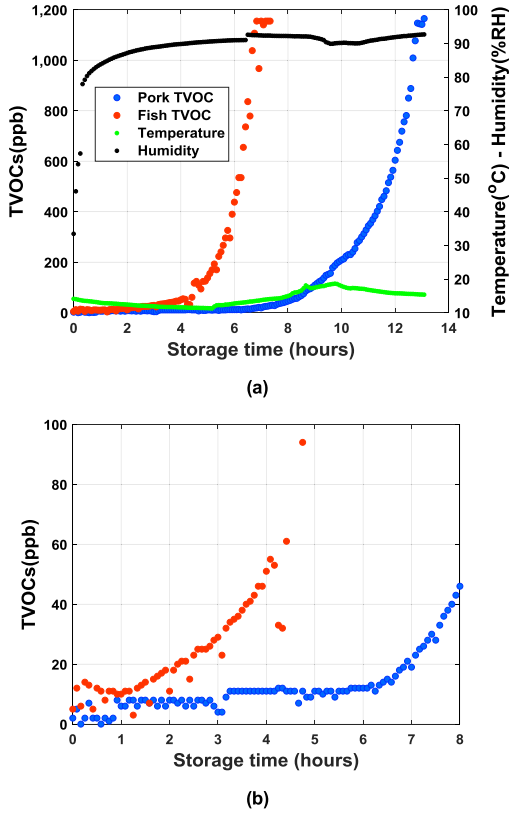

FIGURE 8. Food quality monitoring results at ambient temperature: (a) The TVOC variations after 14 hours of storage. The green and black curves are the storage temperature (°C) and relative humidity (%RH), respectively. The blue and orange curves represent the TVOCs (ppb) released by the pork and fish samples, respectively; (b) The monitored data during the first 8 hours of storage.

Accordingly, the fresh pork chops are considered to be safe when being kept refrigerated (4 °C) in up to 5 days, while that limit for fish is 2 days.

Upon consideration of the FDA recommendations and our observations, we proposed labeling four states of food quality with respect to the storage time as listed in Table 2. Only the monitored data of the refrigerated samples were investigated in this experiment.

TABLE 2. Definition of four states of food quality and their variation rates of the TVOCs.

State	Pork		Fish	
	Duration (hr)	Rate (ppb/hr)	Duration (hr)	Rate (ppb/hr)
Fresh	First 4 hours	0.25	First 4 hours	1.25
Edible	Following 103	1.08	Following 50	3.08
Cautious	Following 61	8.62	Following 32	16.5
Rotten	Final 32	16.72	Final 20	25.3

As previously mentioned, one of the benefits of CNN is that the network not only considers the scalar values of the inputs but also can extract meaningful information from the variation of the input data. Therefore, it is more beneficial to compare the variation rates of the selected feature, the TVOCs, from pork and fish samples. Table 2 also shows the average rates corresponding to four states of food quality.

III. RESULTS

A. FOOD DEMONSTRATION RESULTS

Figures 8 and 9 report the monitored data under ambient and refrigerated storage conditions, respectively, from the demonstration described in Section II.B. In all cases, it was shown that the TVOCs exponentially increased while the other indicators, temperature and humidity, were fairly stable. At ambient temperature, the TVOCs rapidly increased only after a few hours of monitoring (2 hours in the fish case and 6 hours in the pork case), while this duration was 20 and 80 hours in fish and pork cases, respectively, at refrigerator temperature. These variations expressed the compatibility with the findings in [40], [41] that food deterioration gradually released a variety of volatile gases. Additionally, it could be observed that when refrigerated, the TVOCs increased much slower than those under ambient conditions. As widely known in previous works where the temperature was used as an indicator of food quality [38], it was concluded that the quality of food decreased more rapidly at a higher temperature. Our results, hence, showed the reliability of the TVOC-related food quality indicator.

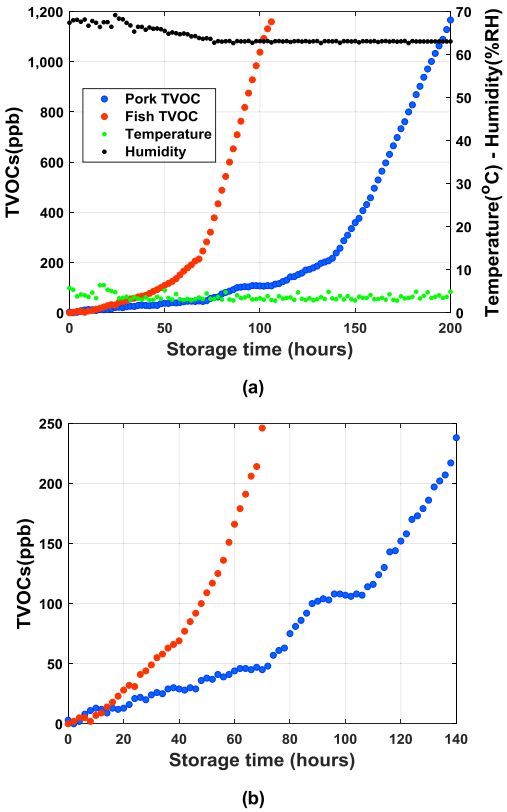

FIGURE 9. Food quality monitoring results at refrigerator temperature: (a) The TVOC variations after 200 hours of storage, equivalent to 8 days. The green and black curves are the storage temperature (°C) and relative humidity (%RH), respectively. The blue and orange curves represent the TVOCs (ppb) released by the pork and fish samples, respectively; (b) The monitored data during the first 140 hours of storage, equivalent to 6 days.

B. CLASSIFICATION RESULTS

In this paper, we systematically compared the classification performance of the three proposed classifiers. The 1-D CNN model took an array of TVOCs within a period of n-minutes as its inputs. With the data sampling rate of approximately 5 minutes (Section II.B), we chose $n = 15$; hence each input sample of the network contained 3 TVOC values. On the contrary, an input sample of the MLP or SVM model was a two-scalar input including one TVOC and one temperature values. Table 3 shows the numbers of input samples of these models. Testing datasets were chosen at 33.3% of the total input samples (three-fold cross-validation) for all models. All models were developed and trained using Python.

TABLE 3. The numbers of input samples of three classification models.

State	CNN model		MLP and SVM models	
	Pork	Fish	Pork	Fish
Fresh	16	16	25	25
Edible	412	196	618	294
Cautious	248	128	365	192
Rotten	124	82	193	124

Figures 10 and 11 show the classification performance of both the CNN and MLP models in terms of loss versus epochs. Both models were trained in 5,000 epochs for comparison. We observed that the 1-D CNN well trained the data of the pork experiment while it was overfitting slightly in the case of fish data since the epoch 1,000th. Similarly, the learning process of the two-scalar MLP showed the same behaviors between the test and the validation curves until the epoch 3,000th, approximately, in both pork and fish cases. In general, the classification performance of these models showed that such numbers of data samples, collected by the RF-powered sensor mote, were sufficient for training the proposed classifiers.

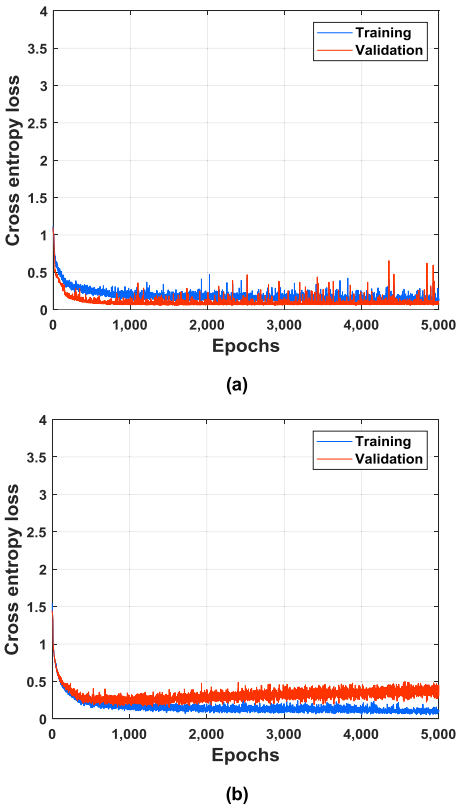

FIGURE 10. Classification performance of the 1-D CNN model: a) in pork case, (b) in fish case.

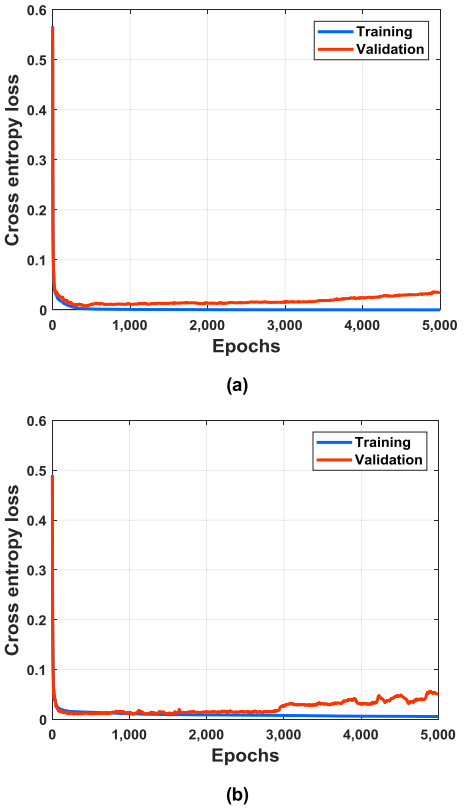

FIGURE 11. Classification performance of the 2-D MLP model: a) in pork case, (b) in fish case.

The overall accuracy of these models was investigated through confusion matrix, the most commonly used metric for classification performance [42]. A confusion matrix is a two-dimensional matrix, of which one dimension is the actual class of an object (target class) and the other is the class predicted by the model (output class). Figure 12 shows the confusion matrixes of the three proposed classifiers.

For comparison, we compared the accuracy among each classifier in Table 4. The MLP model with two-scalar inputs achieved the highest accuracy that was 99% using pork data

TABLE 4. Classification accuracy from each classifier.

Classification accuracy (%)	CNN model	MLP model	SVM model
Pork	97.9	99	83
Fish	90.6	93.3	75

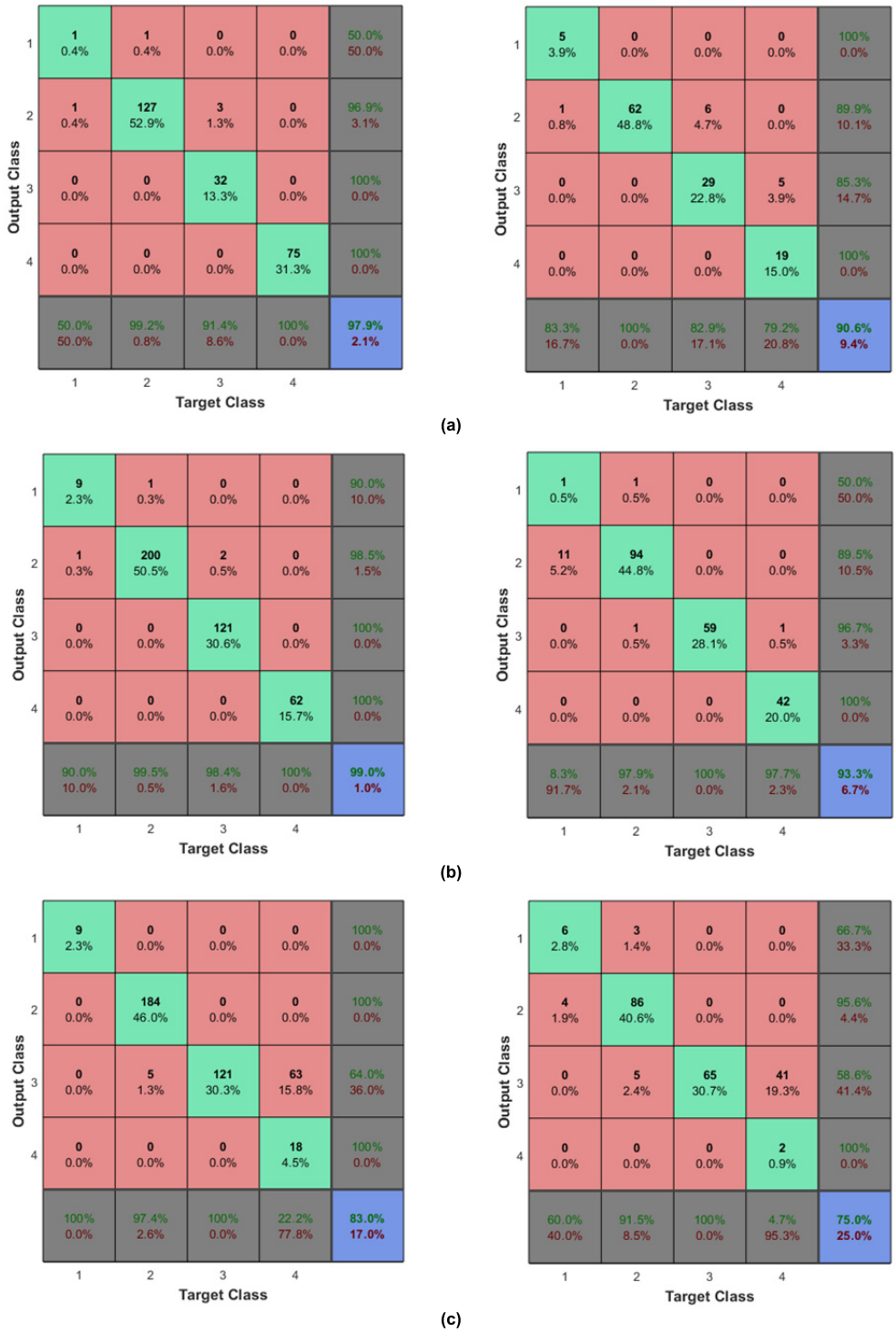

FIGURE 12. Confusion matrix by: (a) the CNN, (b) the MLP, and (c) the SVM models. The left and right figures are the results using pork and fish data, respectively.

and 93.3% using fish data, respectively. The CNN classifier using 1-D inputs obtained the second-highest accuracy of 97.9% and 90.6% with pork and fish data, respectively. The remaining model, SVM, yielded the lowest accuracy of food quality classification.

IV. DISCUSSION AND CONCLUSIONS

The first conclusion came from the demonstration of the RF-powered food quality tracking system. From the investigation in Table 2, it was shown that the TVOCs were released at different rates in different statuses of food quality. The longer the

food was stored, the higher the variation rate of TVOCs was. Also, the TVOCs by fish experiment apparently increased much faster than by pork at the same storage condition. This was expected because the texture of fish meat is less firm than that of pork meat [2], hence it is quicker for fish meat to be decomposed. Additionally, the results of the food demonstration showed that the increased release of volatile gases during the meat spoilage, which could be detected by a single VOC gas sensor, was a reliable indicator to determine food quality. Therefore, the investigation denoted the reliability of the proposed non-invasive method using the TVOC indicator to track food quality.

The study also showed that the far-field RF energy harvesting technology was appropriate for this detection method. With three different operational modes of the sensor module, the average power consumption of the sensor mote was optimized for its self-powering operation. The experimental results affirmed that the proposed RF-powered food quality tracking system was able to operate six times, without the need for external power, before the harvested power drained off at one time of harvesting energy.

One major contribution of the study was the results of food quality classification using the three proposed classifiers. Particularly, this study investigated the employment of CNN using a 1-D feature to predict multi-states of food quality. Although the best performance was not obtained by the CNN model (Table 4), the classification results have reflected the advantage of CNN that it can extract the meaningful data, both the absolute values and their variation information, from the array of TVOCs. In other words, it takes into account the trend of TVOC data without performing the derivative of the data, which the two other algorithms, MLP and SVM, are not able to do without pre-processing the input data.

Another advantage of the CNN, compared to the MLP classifier, is that it can handle any types of data: one-, two-, or three-dimensional data, using kernel filters to sweep over the input dataset. On the contrary, the MLP model must be re-structured and re-trained whenever the input feature is changed to fit the new input dataset.

With the last investigated technique, SVM, the CNN yielded significantly higher accuracy than that of the SVM. In addition, the SVM showed a disadvantage for the multi-class problem due to a large number of the required binary SVM classifiers. In the paper, six binary classifiers were used to train the data, leading to much more computational time and resources. As a result, the proposed one-dimensional CNN is highly appropriate for the challenge of multi-class food quality estimation that requires only one feature, which is the principle of the introduced food spoilage detection method.

Finally, it was realized through the study that the RF-powered tracking system based on the TVOC indicator was highly feasible in food monitoring. Additionally, other possible applications can be benefited from the proposed techniques, such as wearable biosensor devices to track and monitor human health (skin moisture, exhaled breath, etc.), or portable devices to monitor air quality. Flexible antennas and state-of-the-art CMOS technologies can be further applied to reduce the size and cost of the proposed sensor mote, providing more opportunity for the proposed method to be used in the real world. For data analysis, the 1-D CNN model was beneficial in processing the time-varying TVOC signal to yield a good classification of food freshness. Further studies will be conducted to investigate the determination of pork meat and fish meat based on TVOCs under different storage conditions.

REFERENCES

[1] WHO. *Food Safety*. Accessed: Oct. 31, 2017. [Online]. Available: https://www.who.int/news-room/fact-sheets/detail/food-safety
[2] J.-H. Cheng, D.-W. Sun, Z. Han, and X.-A. Zeng, "Texture and structure measurements and analyses for evaluation of fish and fillet freshness quality: A review," *Comprehensive Rev. Food Sci. Food Saf.*, vol. 13, no. 1, pp. 52–61, Jan. 2014.
[3] M. Nemati, A. Hamidi, S. Maleki Dizaj, V. Javaherzadeh, and F. Lotfipour, "An overview on novel microbial determination methods in pharmaceutical and food quality control," *Adv. Pharmaceutical Bull.*, vol. 6, no. 3, pp. 301–308, Sep. 2019.
[4] A. Bajwa, S. Tan, R. Mehta, and B. Bahreyni, "Rapid detection of viable microorganisms based on a plate count technique using arrayed microelectrodes," *Sensors*, vol. 13, no. 7, pp. 8188–8198, Jun. 2013.
[5] J. H. J. Huis in't Veld, "Microbial and biochemical spoilage of foods: An overview," *Int. J. Food Microbiology*, vol. 33, no. 1, pp. 1–18, Nov. 1996.
[6] G. M. ElMasry and S. Nakauchi, "Image analysis operations applied to hyperspectral images for non-invasive sensing of food quality—A comprehensive review," *Biosystems Eng.*, vol. 142, pp. 53–82, Feb. 2016.
[7] F. Gruber, P. Wollmann, W. Grählert, and S. Kaskel, "Hyperspectral imaging using laser excitation for fast Raman and fluorescence hyperspectral imaging for sorting and quality control applications," *J. Imag.*, vol. 4, no. 10, p. 110, 2018.
[8] A. Loutfi, S. Coradeschi, G. K. Mani, P. Shankar, and J. B. B. Rayappan, "Electronic noses for food quality: A review," *J. Food Eng.*, vol. 144, pp. 103–111, Jan. 2015.
[9] G. Comi, "Spoilage of meat and fish," in *The Microbiological Quality of Food: Foodborn Spoilers* New Delhi, India: Woodhead, 2017, pp. 179–210.
[10] O. Fraser and S. Sumar, "Compositional changes and spoilage in fish an introduction," *Nutrition Food Sci.*, vol. 98, no. 5, pp. 275–279, Oct. 1998.
[11] S. Sudevalayam and P. Kulkarni, "Energy harvesting sensor nodes: Survey and implications," *IEEE Commun. Surveys Tuts.*, vol. 13, no. 3, pp. 443–461, 3rd Quart., 2011.
[12] E. da Costa, N. de Oliveira, F. Morais, P. Carvalhaes-Dias, L. Duarte, A. Cabot, and J. Siqueira Dias, "A self-powered and autonomous fringing field capacitive sensor integrated into a micro sprinkler spinner to measure soil water content," *Sensors*, vol. 17, no. 3, p. 575, Mar. 2017.
[13] P. C. Dias, F. J. O. Morais, M. B. de Morais Franca, E. C. Ferreira, A. Cabot, and J. A. Siqueira Dias, "Autonomous multisensor system powered by a solar thermoelectric energy harvester with ultralow-power management circuit," *IEEE Trans. Instrum. Meas.*, vol. 64, no. 11, pp. 2918–2925, Nov. 2015.
[14] P. Carvalhaes-Dias, A. Cabot, and J. Siqueira Dias, "Evaluation of the thermoelectric energy harvesting potential at different latitudes using solar flat panels systems with buried heat sink," *Appl. Sci.*, vol. 8, no. 12, p. 2641, 2018.
[15] J. Silva-Leon, A. Cioncolini, M. R. A. Nabawy, A. Revell, and A. Kennaugh, "Simultaneous wind and solar energy harvesting with inverted flags," *Appl. Energy*, vol. 239, pp. 846–858, Apr. 2019.
[16] M. Mariello, F. Guido, V. M. Mastronardi, M. T. Todaro, D. Desmaále, and M. De Vittorio, "Nanogenerators for harvesting mechanical energy conveyed by liquids," *Nano Energy*, vol. 57, pp. 141–156, Mar. 2019.
[17] T. Soyata, L. Copeland, and W. Heinzelman, "RF energy harvesting for embedded systems: A survey of tradeoffs and methodology," *IEEE Circuits Syst. Mag.*, vol. 16, no. 1, pp. 22–57, 2016.
[18] C. R. Valenta and G. D. Durgin, "Harvesting wireless power: Survey of energy-harvester conversion efficiency in far-field, wireless power transfer systems," *IEEE Microw. Mag.*, vol. 15, no. 4, pp. 108–120, Jun. 2014.

[19] P. V. Nikitin, K. V. S. Rao, R. Martinez, and S. F. Lam, "Sensitivity and impedance measurements of UHF RFID chips," *IEEE Trans. Microw. Theory Techn.*, vol. 57, no. 5, pp. 1297–1302, May 2009.
[20] H. Nakamoto, D. Yamazaki, T. Yamamoto, H. Kurata, S. Yamada, K. Mukaida, T. Ninomiya, T. Ohkawa, S. Masui, and K. Gotoh, "A passive UHF RF identification CMOS tag IC using ferroelectric RAM in 0.35-μm technology," *IEEE J. Solid-State Circuits*, vol. 42, no. 1, pp. 101–110, Jan. 2007.
[21] K. Choi, G. Fazekas, and M. Sandler, "Automatic tagging using deep convolutional neural networks," 2016, *arXiv:1606.00298*. [Online]. Available: http://arxiv.org/abs/1606.00298
[22] Y. Lecun, L. Bottou, Y. Bengio, and P. Haffner, "Gradient-based learning applied to document recognition," *Proc. IEEE*, vol. 86, no. 11, pp. 2278–2324, Nov. 1998.
[23] A. Krizhevsky, I. Sutskever, and G. E. Hinton, "ImageNet classification with deep convolutional neural networks," *Commun. ACM*, vol. 60, no. 6, pp. 84–90, May 2017.
[24] H. Cecotti, "A time–frequency convolutional neural network for the offline classification of steady-state visual evoked potential responses," *Pattern Recognit. Lett.*, vol. 32, no. 8, pp. 1145–1153, Jun. 2011.
[25] N.-S. Kwak, K.-R. Müller, and S.-W. Lee, "A convolutional neural network for steady state visual evoked potential classification under ambulatory environment," *PLoS ONE*, vol. 12, no. 2, 2017, Art. no. e0172578.
[26] J. A. Benediktsson, P. H. Swain, and O. K. Ersoy, "Neural network approaches versus statistical methods in classification of multisource remote sensing data," *IEEE Trans. Geosci. Remote Sens.*, vol. 28, no. 4, pp. 540–552, Jul. 1990.
[27] M. W. Gardner and S. R. Dorling, "Artificial neural networks (the multilayer perceptron)—A review of applications in the atmospheric sciences," *Atmos. Environ.*, vol. 32, nos. 14–15, pp. 2627–2636, Aug. 1998.
[28] R. G. Brereton and G. R. Lloyd, "Support Vector Machines for classification and regression," *Analyst*, vol. 135, no. 2, pp. 230–267, 2010.
[29] T.-H. Nguyen, D.-L. Yang, and W.-Y. Chung, "A high-rate BCI speller based on eye-closed EEG signal," *IEEE Access*, vol. 6, pp. 33995–34003, 2018.
[30] M. Pinuela, P. D. Mitcheson, and S. Lucyszyn, "Ambient RF energy harvesting in urban and semi-urban environments," *IEEE Trans. Microw. Theory Techn.*, vol. 61, no. 7, pp. 2715–2726, Jul. 2013.
[31] F. Alimenti and L. Roselli, "Theory of zero-power RFID sensors based on harmonic generation and orthogonally polarized antennas," *Prog. Electromagn. Res.*, vol. 134, pp. 337–357, 2013.
[32] Z. Popović, S. Korhummel, S. Dunbar, R. Scheeler, A. Dolgov, R. Zane, E. Falkenstein, and J. Hagerty, "Scalable RF energy harvesting," *IEEE Trans. Microw. Theory Techn.*, vol. 62, no. 4, pp. 1046–1056, Apr. 2014.
[33] F. Congedo, G. Monti, L. Tarricone, and V. Bella, "A 2.45-GHz vivaldi rectenna for the remote activation of an end device radio node," *IEEE Sensors J.*, vol. 13, no. 9, pp. 3454–3461, Sep. 2013.
[34] J. F. Dickson, "On-chip high-voltage generation in MNOS integrated," *IEEE J. Solid-State Circuits*, vol. SC-11, pp. 374–378, Jun. 1976.
[35] *Ultra Low Power Boost Converter With Battery Management for Energy*, Dallas, TX, USA: Texas Instruments, 2013.
[36] *Ultra-Low Power Digital Gas Sensor for Monitoring Indoor Air Quality*, Ams AG, Premstätten, Austria Feb. 2019.
[37] GS1. (Apr-2015). *EPCglobal Gen2 Specification*. [Online]. Available: https://www.gs1.org/sites/default/files/docs/epc/Gen2_Protocol_Standard.pdf
[38] P. S. Taoukis and T. P. Labuza, "Reliability of time-temperature indicators as food quality monitors under nonisothermal conditions," *J. Food Sci.*, vol. 54, no. 4, pp. 789–792, Jul. 1989.
[39] FDA. (Mar. 2018). *Refrigerator & Freezer Storage Chart*. [Online]. Available: https://www.fda.gov/downloads/food/resourcesforyou/healtheducators/ucm109315.pdf
[40] W. Lindinger, A. Hansel, and A. Jordan, "On-line monitoring of volatile organic compounds at pptv levels by means of proton-transfer-reaction mass spectrometry (PTR-MS) medical applications, food control and environmental research," *Int. J. Mass Spectrometry Ion Processes*, vol. 173, no. 3, pp. 191–241, Feb. 1998.
[41] P. I. Zakrys, S. A. Hogan, M. G. O'Sullivan, P. Allen, and J. P. Kerry, "Effects of oxygen concentration on the sensory evaluation and quality indicators of beef muscle packed under modified atmosphere," *Meat Sci.*, vol. 79, no. 4, pp. 648–655, Aug. 2008.
[42] K. Ting, "Confusion matrix," in *Encyclopedia of Machine Learning and Data Mining*, C. Sammut and G. I. Webb, Eds. Boston, MA, USA: Springer, 2017.

MINH BINH LAM received the B.E. degree in electrical–electronics engineering from Bach Khoa University, Vietnam, in 2002, and the M.S. degree in telecommunication and information systems from the University of Essex, U.K., in 2004. She is currently pursuing the Ph.D. degree with the Department of Electronic Engineering, Pukyong National University, Busan, South Korea. She is also a Lecturer at the Faculty of Electrical Engineering Technology, Industrial University of Ho Chi Minh City, Vietnam. Her current research interests include high-frequency radio frequency identification, far field communication, and low-power sensor networking.

TRUNG-HAU NGUYEN received the B.E. degree in mechatronics engineering from Bach Khoa University, Vietnam, in 2008, and the M.E. degree in biomedical engineering and the Ph.D. degree in electronic engineering from Pukyong National University, Busan, South Korea, in 2015 and 2020, respectively. His research interests include the development of wearable healthcare sensors, signal processing, and electroencephalogram-based driver-assistance systems.

WAN-YOUNG CHUNG (Senior Member, IEEE) received the B.S. and M.S. degrees in electronic engineering from Kyungpook National University, Daegu, South Korea, in 1987 and 1989, respectively, and the Ph.D. degree in sensor engineering from Kyushu University, Fukuoka, Japan, in 1998. He was an Assistant Professor with Semyung University, from 1993 to 1999. He was also an Associate Professor with Dongseo University, from 1999 to 2008. He has been a Full Professor with the Department of Electronic Engineering, Pukyong National University, South Korea, since September 2008. His areas of interest include ubiquitous healthcare, wireless sensor network applications, and gas sensors.